Natural Hazards and Earth System Sciences
Supplementary Information for

Covariance-informed spatiotemporal clustering improves the detection of climate extremes

Hunter Quintal[1], Antonia Sebastian[1], Marc Serre[2], Wiebke Jager[3], Marleen C. de Ruiter[3]

[1]Department of Earth, Marine, and Environmental Sciences, The University of North Carolina at Chapel Hill, Chapel Hill, 27599, USA
[2]Department of Environmental Sciences and Engineering, The University of North Carolina at Chapel Hill, Chapel Hill, 27599, USA
[3]Institute for Environmental Studies, Vrije Universiteit Amsterdam, Amsterdam, 1081 HV, the Netherlands

Correspondence to: Hunter Quintal (hquintal@email.unc.edu)

Contents of this file

Figures S1 to S7
Tables S1 to S6

Introduction

This Supplementary Information contains six additional figures and three additional tables. Figures S1-S3 and Tables S1-S2 support section 3 (Application) of the main text. Figures S4-S7 and Tables S3-S6 supports section 4 (Results) of the main text.

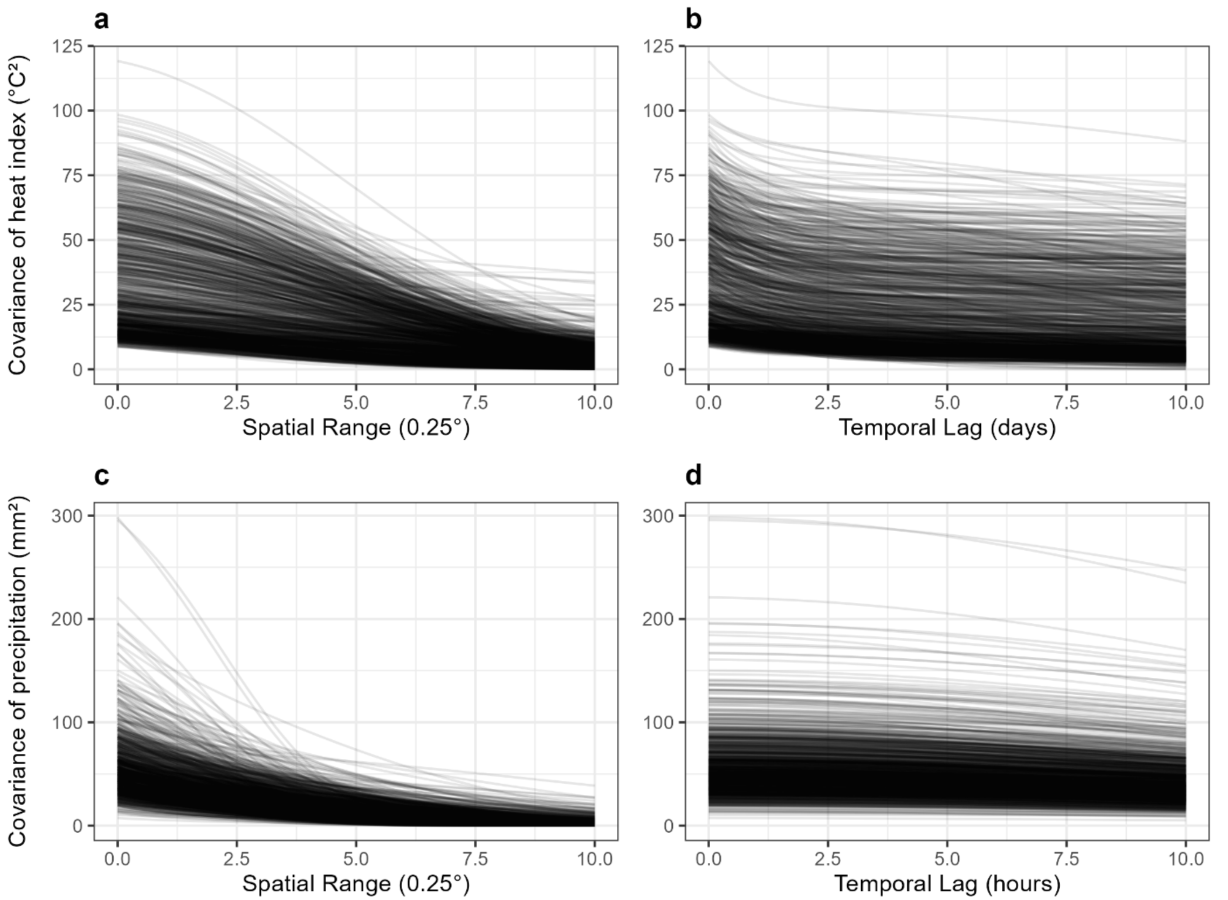

Figure S1. Space time separable covariance models of daily heat index by a) spatial range and b) temporal lag and of hourly precipitation by c) spatial range and d) temporal lag. Each panel includes 1008 covariance models representing every month from 1940 to 2023. Covariance models were fit to experimental covariance estimated using BMElib software. The sill of the covariance represents the sum of all the variances within a data set, representing the overall spread or dispersion of all data points from the mean. A higher sill means the data is more spread out, while a lower sill means the data is closer to the mean. In each panel, the sill of covariance represents the most variability at that location (a, c) and at that time (b, d). This means that a sill of 100° C^2 had at most $\sqrt{100° C^2}$ or 10° C of heat index variability at any given location and at any given time for that month. Similarly, a sill of 100 mm^2 had at most $\sqrt{100\ mm^2}$ or 10 mm of precipitation variability. Months whose sills are relatively low experienced more consistent intensities, while months whose sills are relatively high experienced large intensity swings.

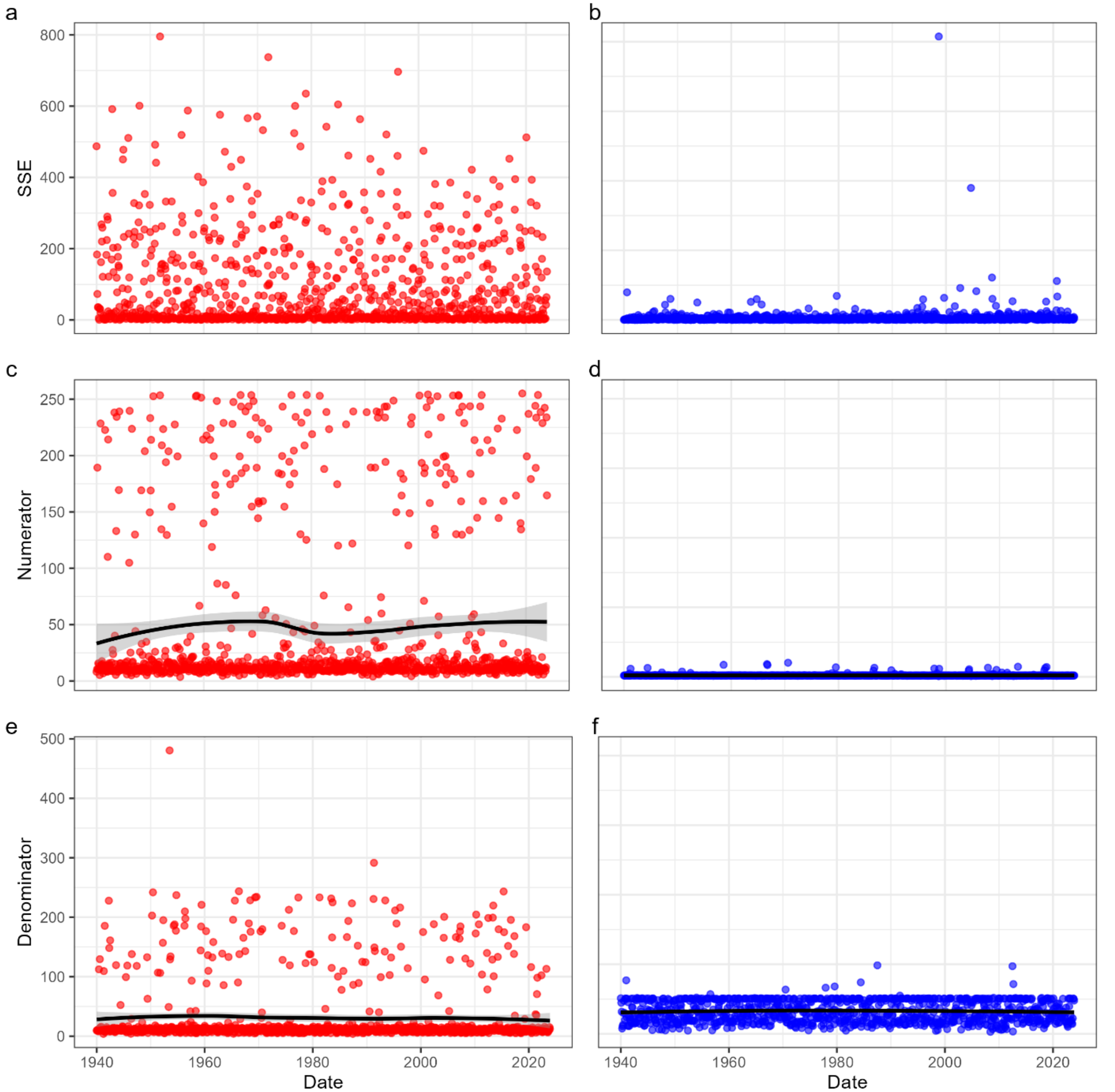

Figure S2. Sum of squared error for monthly covariance models of a) heat index and b) precipitation. Space time metrics were then calculated using monthly covariance models illustrated in Fig. S1. In calculating a space time metric using Eq. (3), both a numerator (panels c and d) and a denominator (panels e and f) are derived, which represent the relative persistence of a variable in space and time, respectively. The sum of squared error is greater for heat index (a) than for precipitation (b), indicating that the covariance of daily heat index fluctuates significantly more than that of 24-hour precipitation. There is more variation in the numerators and denominators of heat index (c, e) than that of precipitation (d, f). Heat index values are often, however, are bounded between 0 and 250, yielding space time metrics consistently near 1. Conversely, precipitation values are not bounded on the same range, where numerators are near 0 while denominators range between 0 and 50, yielding space time metrics consistently near 0.2.

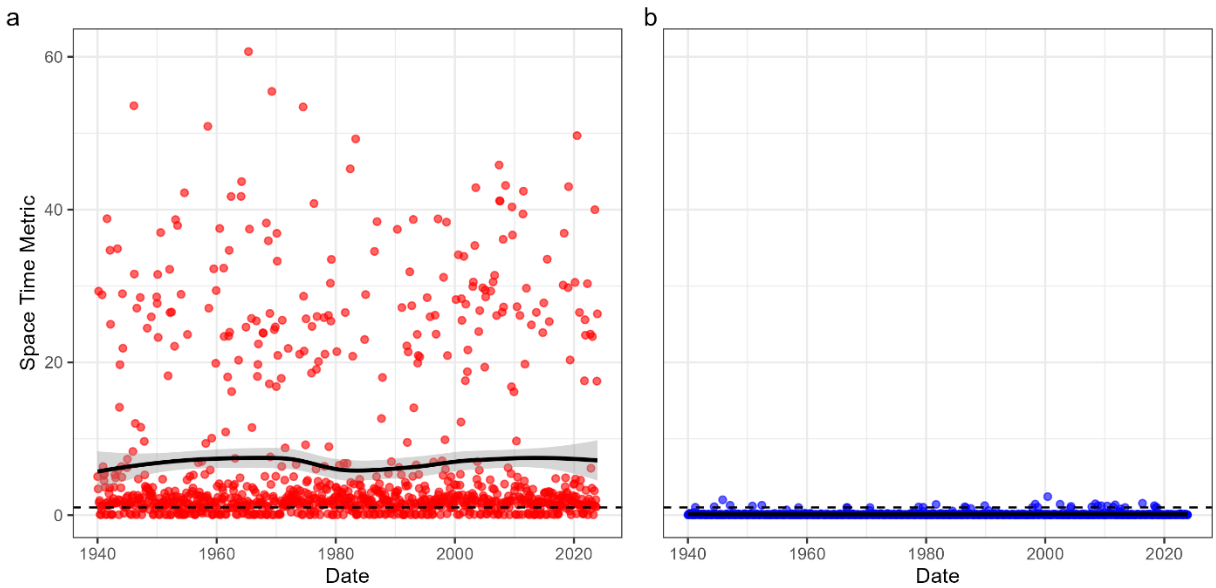

Figure S3. Space time metrics of a) heat index and precipitation b) calculated using the numerators and denominators plotted in Fig. S2. While the metric is stable for precipitation (b), the metric is less consistent for heat index (a), making the space time metric defined using Eq. (3) a less reliable statistic than the space time metric calculated using Eq. (4), which were selected for this analysis and are reported in Fig. 4. Note that a space time metric of one, identified with a horizontal dashed line, indicates that the ERA5 native resolution is appropriate for spatiotemporal clustering.

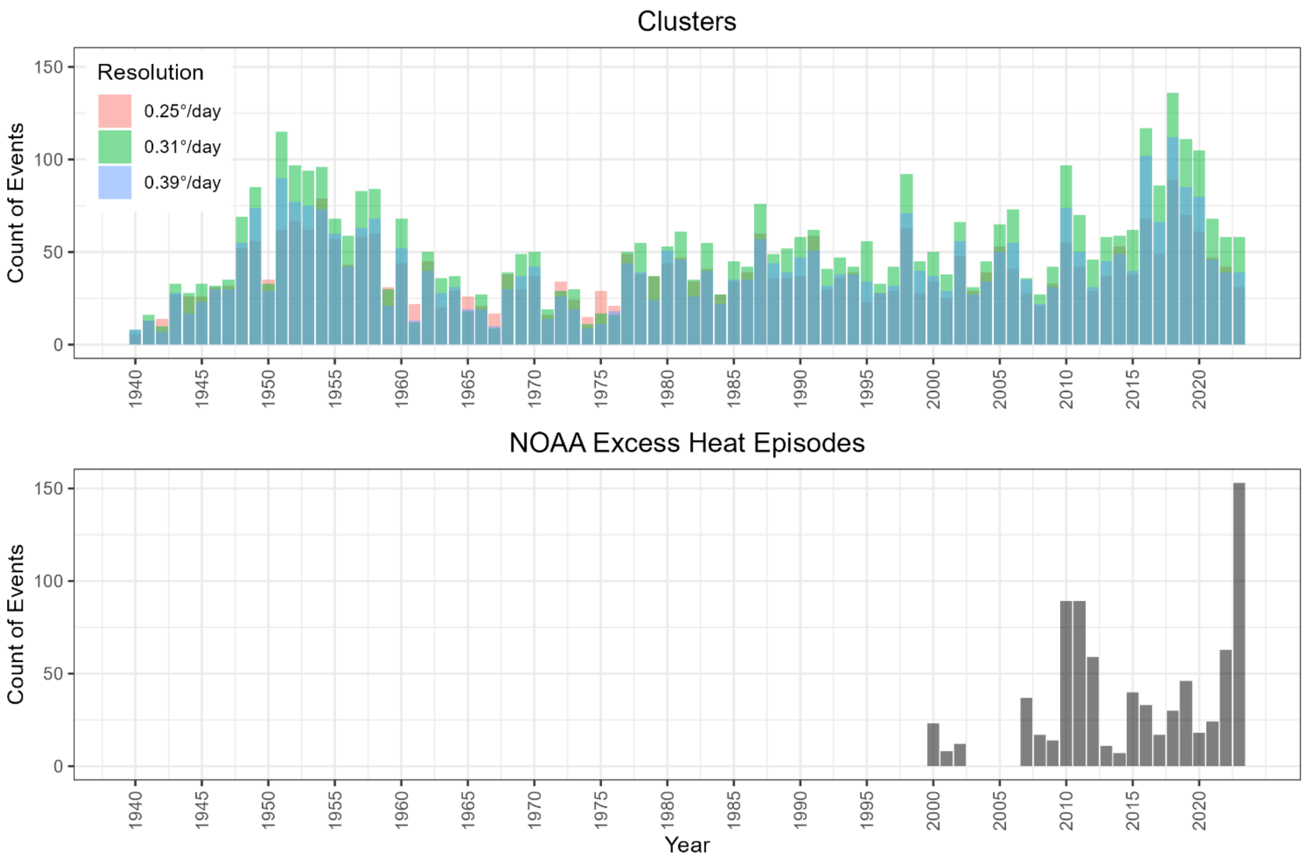

Figure S4. Yearly count of heat index clusters (top) and NOAA excess heat episodes (bottom). Reporting of NOAA excess heat episodes begins in 2000. Clusters are reported separately by each spatial resolution used for spatiotemporal clustering that was determined by covariance analysis. Clusters are more frequently identified using the summer median space time metric (0.31°/day), except in years when few clusters are detected; in this case, the ERA5 native resolution (0.25°/day) identifies the most clusters.

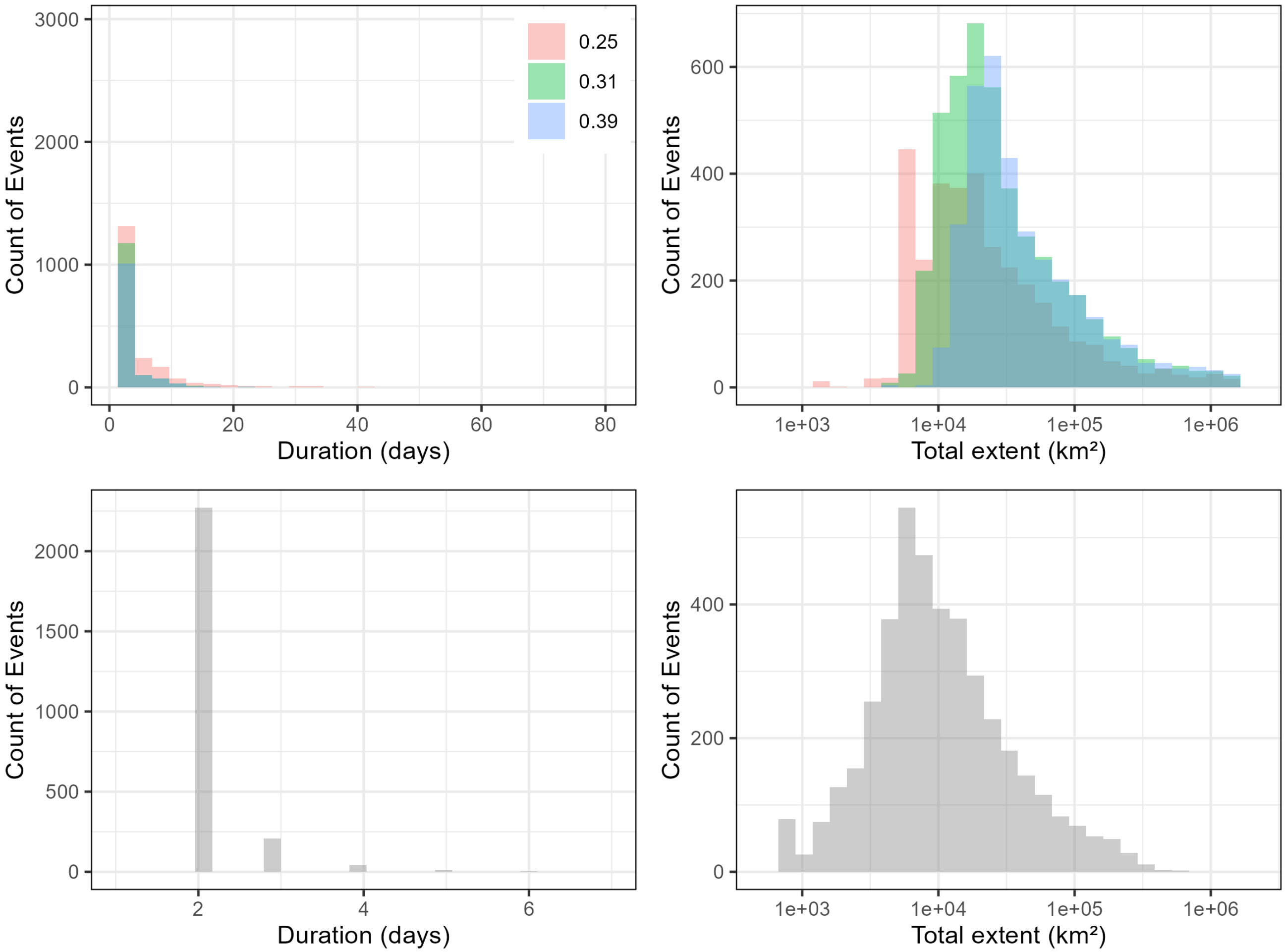

Figure S5. Cluster spatiotemporal duration (left) and extent (right) for heat index (top) and precipitation (bottom). Heat index clusters are reported separately by each spatial resolution used for spatiotemporal clustering that was determined by covariance analysis. Precipitation clusters are reported exclusively for the ERA5 native resolution (0.25°/hour) because the space time metric for precipitation is less than one. Heat index clusters defined using the ERA5 native resolution (0.25°/day) last longer, but cover a smaller area, than the clusters defined using either space time metric. Precipitation clusters tend to last for a shorter period of time and cover a smaller area than heat index clusters.

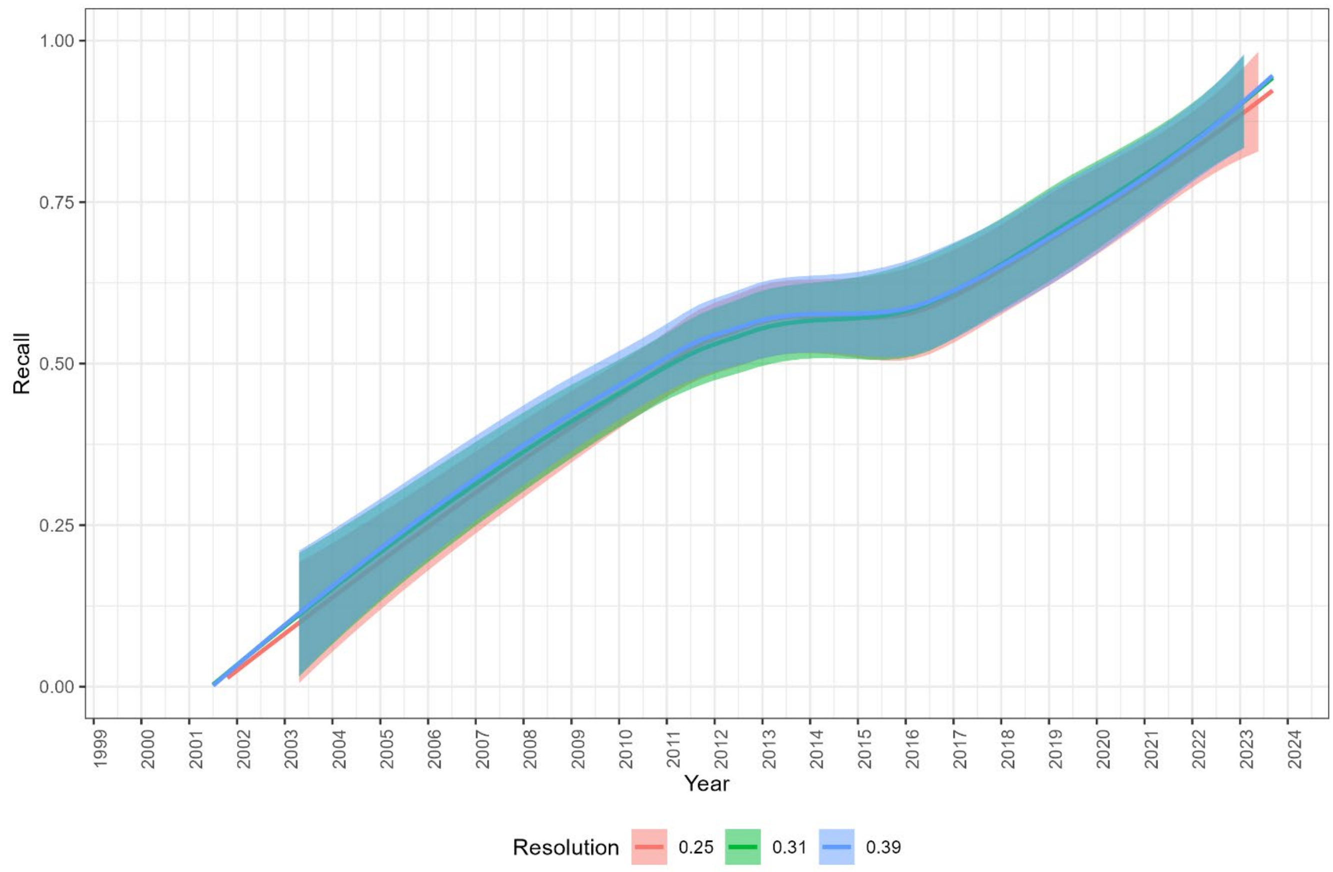

Figure S6. Time series of daily aggregated recall across the Southeastern US (county day units) for NOAA excess heat episodes when compared to clustered heat index events at 0.25° per day (red), 0.31° per day (green), and 0.39° per day (blue). Recall is greatest for both 0.31° and 0.39° per day clusters, but this is not statistically significant. Recall improves over the record, implying that NOAA reporting quality has improved over time.

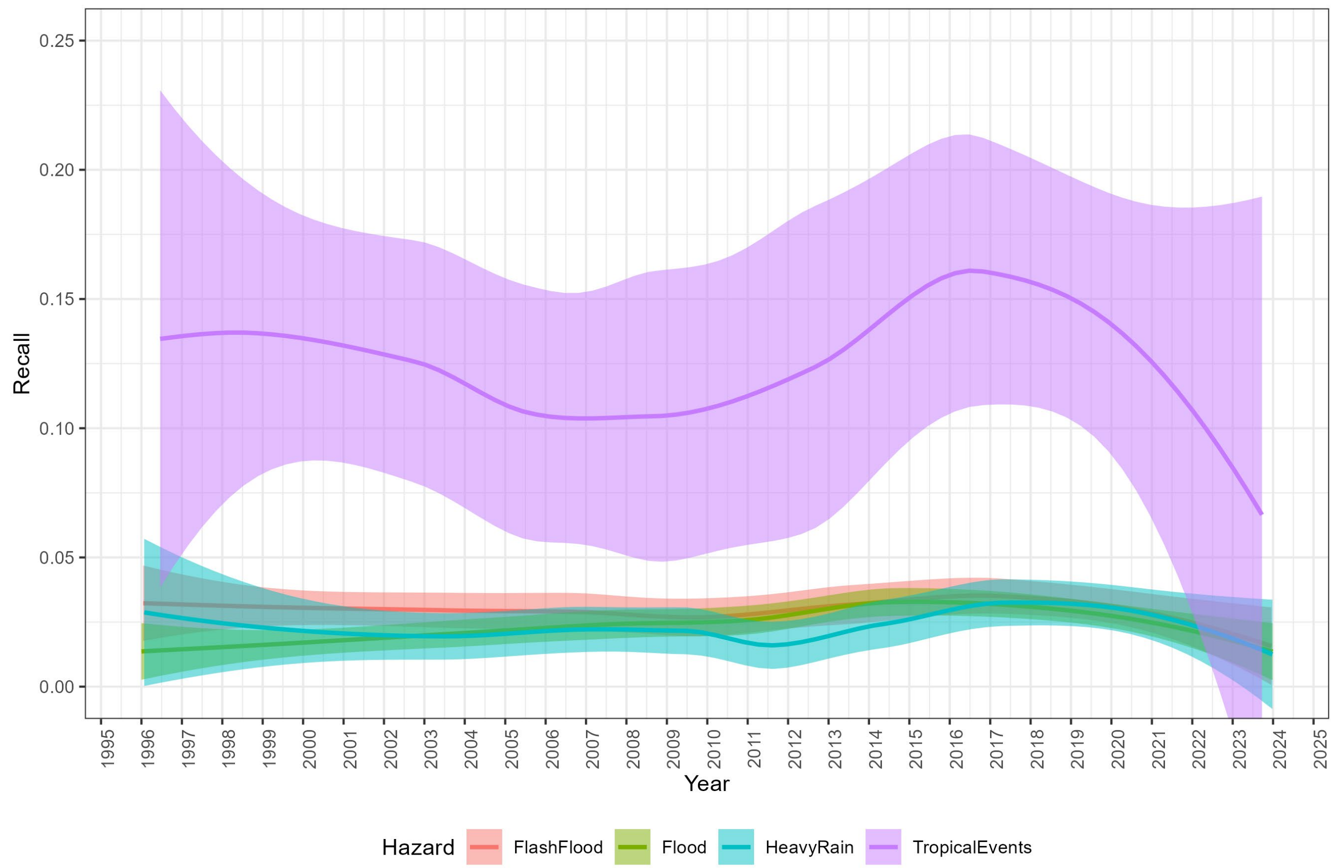

Figure S7. Time series of daily aggregated recall across the Southeastern US (county day units) for NOAA flash flood, flood, heavy rain, and tropical event (hurricane, tropical depression, tropical storm, typhoon) episodes when compared to clustered precipitation events at 0.25° per hour. Recall is greatest for larger, tropical event episodes and poor for flash flood, flood, and heavy rain episodes. Note that the y-axis ranges from 0 to 0.25, which is nowhere near a perfect recall of 1.

Table S1. Count of NOAA storm episodes across the CONUS region (1996-2023) and then subset to the Southeast (1996-2023 and 2019-2023 [the validation period for this study]).

NOAA Storm	CONUS	Southeast	Southeast
Time Period	1996 – 2023	1996 – 2023	2019 – 2023
Excess heat	1,124	790	340
Flash flood	37,957	18,085	2,460
Flood	18,988	8,952	1,615
Heat	2,605	1,920	455
Heavy rain	8,072	3,339	486
Hurricane	28	25	17
Tropical depression	48	43	23
Tropical storm	594	525	116
Typhoon	141	139	0

Table S2. Computational processing time to calculate experimental covariance using BMElib with 5,040 spatial observations per temporal layer. Note that hourly precipitation grouped annually exceeded the computational capacity of a desktop machine.

Variable	Resolution	Aggregation	Layers (n)	Processing time (hr)
Heat Index	Day	Month	31	84.0
		Year	365	117.6
Precipitation	Hour	Month	744	151.2
		Year	8,760	NA

Table S3. Aggregated recall of NOAA episodes between the native ERA5 resolution and the covariance-informed space time cube across the Southeastern US from 2019 to 2023. Note that a resolution of 0.05° is defined by the record median of the precipitation space time metric, which is not possible to obtain from the ERA5 reanalysis product. Note also that the resolutions of 0.31° and 0.39° are only applied to heat index and so the calculation of recall at these resolutions against precipitation hazards is not relevant.

Resolution	Excess heat	Flash flood	Flood	Heat	Heavy rain	Hurricane	Trop. depression	Trop. storm
0.05°	-	-	-	-	-	-	-	-
0.25°	0.919	0.038	0.033	0.642	0.055	0.333	0.033	0.089
0.31°	0.940	-	-	0.692	-	-	-	-
0.39°	0.945	-	-	0.707	-	-	-	-

Table S4. Confusion matrix for heat index clusters derived from the native ERA5 resolution. Units are county-days.

Resolution: 0.25° per day (2019-2023)		NOAA Excess Heat Episodes	
		Presence	Absence
Clusters	Presence	6,192	68,685
	Absence	541	2,978,213

Table S5. Confusion matrix for ERA5-derived heat index resampled by the space time metric summer median prior to clustering. Units are county-days.

Resolution: 0.31° per day (2019-2023)		NOAA Excess Heat Episodes	
		Presence	Absence
Clusters	Presence	6,169	77,400
	Absence	397	2,459,681

Table S6. Confusion matrix for ERA5-derived heat index resampled by the space time metric record median prior to clustering. Units are county-days.

Resolution: 0.39° per day (2019-2023)		NOAA Excess Heat Episodes	
		Presence	Absence
Clusters	Presence	6,143	82,944
	Absence	360	2,425,253